Parametric estimation for Gaussian operator scaling random fields and anisotropy analysis of bone radiograph textures

Hermine Biermé[1], Claude-Laurent Benhamou[2], and Frédéric Richard[1]

1. University Paris Descartes, MAP5 CNRS UMR 8145
[hermine.bierme,frederic.richard]@parisdescartes.fr,
2. INSERM U658, Hospital of Orleans, France. *

Abstract. In this paper, we consider a stochastic anisotropic model for trabecular bone x-ray images. In [1], a fractal analysis based on isotropic Fractional Brownian Fields was proposed to characterize bone microarchitecture. However anisotropy measurement is of special interest for the diagnosis of osteoporosis [7]. We propose to model trabecular bone radiographs by operator scaling Gaussian random fields which are anisotropic generalizations of the Fractional Brownian Field. We construct consistent estimators for these models and apply them on trabecular bone x-ray images. Our first results suggest that these models are relevant for this modeling.

1 Introduction

Texture analysis is a challenging issue of Image Processing, which is often raised in medical applications. There are several types of texture approaches. Among stochastic approaches, fractal analysis has been largely used in medical applications [1, 7, 8, 10]. The stochastic model beyond fractal analysis is the fractional Brownian field (FBF) which is a multi-dimensional extension of the famous fractional Brownian motion implicitly introduced in [17] and defined in [19]. This field is mathematically defined as the unique centered Gaussian field, null at 0 almost surely, with stationary increments, isotropic, and self-similar of order $H \in (0, 1)$. Its variogram is of the form $v(x) = C_H|x|^{2H}, \forall x \in \mathbb{R}^2$, with $|\cdot|$ the Euclidean norm. Parameter H, called the Hurst index, is a fundamental parameter which is an indicator of texture roughness and is directly related to the fractal dimension of the graph sample paths.

FBF was used for the characterization and classification of mammogram density [8], the study of lesion detectability in mammogram textures [12], and the assessment of breast cancer risk [8, 13]. Fractal analysis has also been used for the radiographic characterization of bone architecture and the evaluation of osteoporotic fracture risk [1]. However, it is well-established that the anisotropy

* We are grateful to the ANR french agency for the financial support to the project ANR MATAIM NT09_441552.

of the bone is an important predictor of fracture risk [7]. Hence fractal analysis with fractional Brownian fields (FBF), which are isotropic by definition, is not completely satisfactory for this medical application. In this paper, our aim is to propose a suitable model which accounts properly for the anisotropy of bone radiograph textures.

The study of random field anisotropy is a wide field of research in the Probability Theory. It covers numerous open issues related to the definition and the analysis of anisotropy, the estimation of anisotropic model parameters, and the simulation of anisotropic fields [4, 3, 6, 11, 20]. In [6], A. Bonami and A. Estrade set a generic framework in which it is possible to define numerous types of anisotropic fields. This framework gathers centered Gaussian fields with stationary increments $\{X(x)\,;\, x \in \mathbb{R}^d\}$, null at 0 almost surely, whose variogram v is characterized by a positive even measurable function f satisfying the relation

$$\forall\, x \in \mathbb{R}^d, v(x) = \mathbb{E}\left(X(x)^2\right) = \int_{\mathbb{R}^d} \left|e^{ix\cdot\zeta} - 1\right|^2 f(\zeta)d\zeta \tag{1}$$

and the condition $\int_{\mathbb{R}^d} \left(1 \wedge |\zeta|^2\right) f(\zeta)d\zeta < \infty$. Within this framework, a field is isotropic whenever the so-called spectral density f of the field is radial, and anisotropic when f depends on the direction $\arg(\zeta)$ of ζ.

In [4, 5], we studied 2-dimensional Gaussian fields with spectral density of the form

$$\forall\, \zeta \in \mathbb{R}^2, f(\zeta) = |\zeta|^{-2h(\arg(\zeta))-2}, \tag{2}$$

where h is a measurable π-periodic function with range $[H, M] \subset (0, 1)$ where $H = \operatorname{essinf}_{[-\pi,\pi)} h$ and $M = \operatorname{esssup}_{[-\pi,\pi)} h$. These fields extend FBF, which are obtained when the function h is almost everywhere constant and equal to the Hurst index H. When h is not constant, the function h depends on the orientation and, consequently, the corresponding field is anisotropic. Another extension of FBF, called operator scaling Gaussian random fields [3], can be obtained by taking spectral densities of the form

$$\forall c > 0,\ \ \forall \zeta \in \mathbb{R}^2\,,\ \ f(c^E\zeta) = c^{-2-\mathrm{tr}(E)} f(\zeta), \tag{3}$$

for some real 2×2 matrix E. The spectral density of an FBF with Hurst index $H \in (0, 1)$, given by $f(\zeta) = |\zeta|^{-2H-2}$, for $\zeta \in \mathbb{R}^2$, satisfies (3) for $E = I_2/H$ with I_2 the identity matrix. In such a model, the anisotropy is characterized by the 2×2 parameters of the matrix E.

In this paper, we focus on a particular class of 2-dimensional operator scaling field for which E is a diagonal matrix. More precisely, we consider 2 dimensional Gaussian fields with spectral density of the form

$$\forall\, \zeta = (\zeta_1, \zeta_2) \in \mathbb{R}^2, f(\zeta) = \left(\zeta_1^2 + \zeta_2^{2a}\right)^{-\beta}, \tag{4}$$

where $\beta = H_1 + (1 + 1/a)/2$ and $a = H_2/H_1$ for some $0 < H_1 \leq H_2 < 1$. Then f satisfies (3) for $E = \mathrm{diag}(1/H_1, 1/H_2)$ and 2 dimensional FBFs are obtained when $H_2 = H_1$, which gives the Hurst index. When $H_1 \neq H_2$ the corresponding field is anisotropic.

There are several ways to analyze the anisotropy of a field. One simple way consists of characterizing the Hölder regularity of rectrictions of the field along oriented lines. However, it was shown that the directional regularity (the regularity of these line restrictions) of any 2-parameter Gaussian random field obtained from (1) is constant, except in at most one direction where it can be larger [11]. In particular, the directional regularity of field model (2) is the same whatever the direction. Hence, the anisotropy of such a model cannot be characterized using line restrictions. For such a model, one can rather study the regularity of windowed Radon transforms [6].

In this paper, we show that fields defined by (4) can have a privileged direction where line restrictions are more regular than in other directions. We also propose some techniques for the estimation of parameters H_1 and H_2. Estimators are constructed using line restrictions and following principles of generalized quadratic variations. Finally, adapting results shown in [4], we prove the convergence of these estimators.

In collaboration with L. Benhamou and M. Rachidi (INSERM U658, Orleans, France) [5], we studied trabecular bone x-ray images. After some preliminary experiments, we came to the conclusion that model (2) was not suitable for the modeling of these images. Due to trabecular structures of the bone, these images have a privileged direction which is detectable from the analysis of line regularity. Such a situation is analogous to the one of sedimentary aquifers whose scaling properties vary according to directions and which were successfully modeled by operator scaling fields [2]. In this paper, we present some preliminary experiments suggesting the adequacy of model (4) to bone radiograph textures.

In Section 2, we recall main properties of operator scaling fields and construct consistent estimators for H_1 and H_2. In Section 3, we present results of estimation on trabecular bone x-ray images, which suggest adequacy to this modeling.

2 Main properties

Let X be a Gaussian field with spectral density (GFSD) on $\mathbb{R}^2$ given by (4) for $0 < H_1 \leq H_2 < 1$. Let us denote E the diagonal 2×2 matrix $E = \mathrm{diag}(1/H_1, 1/H_2)$. We note $q = \mathrm{tr}(E)$ and remark that

$$q = 1/H_1 + 1/H_2 = (1 + 1/a)/H_1,$$

with $a = H_2/H_1 \geq 1$ such that $\beta = H_1\,(1 + q/2)$.

2.1 Operator scaling property

Let us define $\psi(\zeta) = \left(\zeta_1^2 + \zeta_2^{2a}\right)^{H_1/2}$, for $\zeta \in \mathbb{R}^2$, such that ψ is continuous on $\mathbb{R}^2$ with positive values on $\mathbb{R}^d \setminus \{0\}$ and satisfies $\psi(0) = 0$ and $\psi(c^E\zeta) = c\psi(\zeta)$ for all $c > 0$, where c^E is the exponential matrix $c^E = \sum_{n\in\mathbb{N}} \frac{\ln(c)^n}{n!} E^n$. According

to Theorem 4. 1 of [3], the random field X is a Harmonizable operator scaling Gaussian field with respect to E (since $E = E^t$):

$$\forall c > 0, \ \left\{X(c^E x); x \in \mathbb{R}^2\right\} \stackrel{fdd}{=} \left\{cX(x); x \in \mathbb{R}^2\right\},$$

where $\stackrel{fdd}{=}$ means equality for finite dimensional distributions. The operator scaling property is an anisotropic generalization of the well-known self-similarity property.
In particular, for $H_1 = H_2$, the random field X is self-similar of order $H = \min(H_1, H_2)$, which means that

$$\forall c > 0, \ \left\{X(cx); x \in \mathbb{R}^2\right\} \stackrel{fdd}{=} \left\{c^H X(x); x \in \mathbb{R}^2\right\}, \forall c > 0.$$

Moreover, in this case, the spectral density is a radial function, which implies that X is isotropic. Being Gaussian, with stationary increments, null at point zero almost surely, self-similar of order H and isotropic is enough to conclude that X is the famous FBF of Hurst index H. Then, any restriction along straight lines

$$X_{\theta,x_0} = \{X(x_0 + t\theta) - X(x_0) \ ; \ t \in \mathbb{R}\}, \tag{5}$$

for a point $x_0 \in \mathbb{R}^2$ and a unit vector $\theta = (\theta_1, \theta_2)$, will also be a fractional Brownian motion (1 dimensional process) of index H.
When $H_1 \neq H_2$, the stationarity of increments and the operator scaling property with respect to the diagonal matrix E lead to the fact that for any $x_0 \in \mathbb{R}^2$, processes X_{θ,x_0} are fractional Brownian motion of index H_1 when $\theta_2 = 0$ and H_2 when $\theta_1 = 0$. Note that in any other direction θ with $\theta_1 \neq 0$ and $\theta_2 \neq 0$, processes X_{θ,x_0} are not self-similar. Therefore self-similarity parameters are too restrictive to characterize those processes. However, these parameters considered at small scales, are closely linked to Hölder regularity index as we will see in the next section.

2.2 Regularity

Using Kolmogorov-Centsov criterion [15], one can prove that $H = \min(H_1, H_2)$ is the critical Hölder exponent of X. This means that for any $\alpha \in (0, H)$, sample paths of X satisfy a uniform Hölder condition of order α on $[-T, T]^d$, for any $T > 0$: there exists a positive random variable A with $\mathbb{P}(A < +\infty) = 1$ such that

$$\forall x, y \in [-T, T]^d, \quad |X(x) - X(y)| \leq A|x - y|^\alpha; \tag{6}$$

while for any $\alpha \in (H, 1)$, almost surely the sample paths of X fail to satisfy any uniform Hölder condition of order α. We refer to Theorem 5.4 of [3] for the proof of this result. Actually, global Hölder regularity H does not capture the anisotropy of the field. Therefore one can study regularity properties of the field along straight lines, considering critical Hölder exponent of processes defined by (5). This will provide some additional directional regularity information. Note that when X has stationary increments, the Hölder regularity of the process X_{θ,x_0} will not depend on point $x_0 \in \mathbb{R}^2$ so one only has to study the regularity of $\{X(t\theta) \, ; \, t \in \mathbb{R}\}$ for all directions θ. Let us recall Definition 6 of [6].

Definition 1. *Let $\{X(x); x \in \mathbb{R}^d\}$ with stationary increments and let θ be any direction of the unit sphere. If the process $\{X(t\theta); t \in \mathbb{R}\}$ has Hölder critical exponent $\gamma(\theta)$ we say that X admits $\gamma(\theta)$ as directional regularity in direction θ.*

Note that if X is a GFSD given by f, for any direction θ, the process $\{X(t\theta); t \in \mathbb{R}\}$ is still a Gaussian process with spectral density given by the Radon transform of f, namely,

$$\forall p \in \mathbb{R},\ T_\theta f(p) = \int_{\mathbb{R}} f(p\theta + s\theta^\perp) ds, \tag{7}$$

where $(\theta, \theta^\perp)$ is an orthonormal basis of $\mathbb{R}^2$. It is well known that the asymptotic behavior of the spectral density determines the Hölder regularity of the process, as we recall in the sequel. Let us first introduce some notations. For any $H \in (0,1)$, we note $f(\xi) \asymp_{+\infty} |\xi|^{-2H-1}$, if f satisfies: for any $\varepsilon > 0$ there exists $A, B_1, B_2 > 0$ such that for almost all $\xi \in \mathbb{R}$,

$$|\xi| \geq A \ \Rightarrow\ B_2 |\xi|^{-2H-1-\varepsilon} \leq f(\xi) \leq B_1 |\xi|^{-2H-1+\varepsilon}. \tag{8}$$

Remark that $|\xi|^{-2H-1}$ is, up to a constant, the spectral density of a fractional Brownian motion of Hurst index H. In the same vein, for any $H \in (0,1)$, we note $v(y) \asymp_0 |y|^{2H}$, if v satisfies: for any $\varepsilon > 0$ there exists $\delta, C_1, C_2 > 0$ such that for all $y \in \mathbb{R}$,

$$|y| \leq \delta \ \Rightarrow\ C_2 |y|^{2H+\varepsilon} \leq v(y) \leq C_1 |\xi|^{2H-\varepsilon}. \tag{9}$$

We recall here results proved in [6].

Theorem 1. *Let X be a Gaussian process with spectral density f and variogram v. Let $H \in (0,1)$.*
(a) If $f(\xi) \asymp_{+\infty} |\xi|^{-2H-1}$ then $v(y) \asymp_0 |y|^{2H}$.
(b) If $v(y) \asymp_0 |y|^{2H}$ then X admits H as critical Hölder exponent.

In [4] we prove that better estimates on the spectral density enable to give consistent estimators for H. Therefore we give stronger results for spectral densities $T_\theta f$ of line processes $\{X(t\theta)\,;\, t \in \mathbb{R}\}$.

Theorem 2. *Let f be a spectral density given by (4). Let $\theta = (\theta_1, \theta_2)$ be a unit vector of $\mathbb{R}^2$.*
(a) If $\theta_1 \neq 0$ and $\theta_2 \neq 0$, then

$$T_\theta f(p) = |p|^{-2H_1-1} \left(\int_{\mathbb{R}} (s^{2a} + \theta_1^{-2})^{-\beta} ds \right) / |\theta_1| + O_{|p| \to +\infty} \left(|p|^{-2H_1-1-(1-1/a)} \right).$$

(b) If $\theta_2 = 0$, then $T_\theta f(p) = |p|^{-2H_1-1} \left(\int_{\mathbb{R}} (s^{2a}+1)^{-\beta} ds \right)$.
(c) If $\theta_1 = 0$, then $T_\theta f(p) = |p|^{-2H_2-1} \left(\int_{\mathbb{R}} (s^2+1)^{-\beta} ds \right)$.

Proof. Let $\theta = (\theta_1, \theta_2)$, then one can choose $\theta^\perp = (\theta_2, -\theta_1)$ such that

$$T_\theta f(p) = \int_{\mathbb{R}} \left((p\theta_1 + s\theta_2)^2 + (p\theta_2 - s\theta_1)^{2a} \right)^{-\beta} ds.$$

Let us assume that $\theta_1 \neq 0$ and let the change of variables $u = s\theta_1 - p\theta_2$, then

$$T_\theta f(p) = \frac{1}{|\theta_1|} \int_{\mathbb{R}} \left((p/\theta_1 + u\theta_2/\theta_1)^2 + u^{2a} \right)^{-\beta} du. \tag{10}$$

Since $T_\theta f$ is an even function one can assume that $p > 0$ and let the change of variables $u = p^{1/a} s$ such that

$$T_\theta f(p) = \frac{1}{|\theta_1|} p^{1/a - 2\beta} \int_{\mathbb{R}} \left(\left(1/\theta_1 + p^{-(1-1/a)} s\theta_2/\theta_1 \right)^2 + s^{2a} \right)^{-\beta} ds.$$

This concludes for the proof when $\theta_2 = 0$, since $1/a - 2\beta = -1 - 2H_1$. Otherwise, let us consider

$$|\theta_1| p^{-1/a + 2\beta} T_\theta f(p) - \int_{\mathbb{R}} \left(1/\theta_1^2 + s^{2a} \right)^{-\beta} ds = \int_{\mathbb{R}} E_\theta f(p, s) ds,$$

where

$$E_\theta f(p,s) = \left(\left(1/\theta_1 + p^{-(1-1/a)} s\theta_2/\theta_1 \right)^2 + s^{2a} \right)^{-\beta} - \left(1/\theta_1^2 + s^{2a} \right)^{-\beta}.$$

Note that

$$\begin{aligned}
|E_\theta f(p,s)| &\leq \beta p^{-(1-1/a)} |s\theta_2/\theta_1| \int_0^1 \left(\left(1/\theta_1 + t p^{-(1-1/a)} s\theta_2/\theta_1 \right)^2 + s^{2a} \right)^{-\beta - 1/2} dt \\
&\leq \beta p^{-(1-1/a)} |s\theta_2/\theta_1| \left(1/4\theta_1^2 + s^{2a} \right)^{-\beta - 1/2} \text{ if } |s| \leq p^{1-1/a}/2|\theta_2| \\
&\leq \beta p^{-(1-1/a)} |\theta_2/\theta_1| |s|^{-2a(\beta + 1/2) + 1} \text{ if } |s| > p^{1-1/a}/2|\theta_2|.
\end{aligned}$$

Therefore, choosing $p > |2\theta_2|^{1/(1-1/a)}$, one has

$$\begin{aligned}
&\int_{\mathbb{R}} |E_\theta f(p,s)| \, ds \\
&\quad \leq \beta p^{-(1-1/a)} |\theta_2/\theta_1| \left(\int_{\mathbb{R}} |s| \left(1/4\theta_1^2 + s^{2a} \right)^{-\beta - 1/2} ds + \int_{|s|>1} |s|^{-2a(\beta+1/2)+1} ds \right) \\
&= O_{p \to +\infty} \left(p^{-(1-1/a)} \right),
\end{aligned}$$

since $2a(\beta + 1/2) > 2a\beta > 2$. Finally, when $\theta_1 = 0$, we have

$$T_\theta f(p) = \int_{\mathbb{R}} \left(s^2 + p^{2a} \right)^{-\beta} ds.$$

Therefore, the change of variables $s = p^a u$ leads to

$$T_\theta f(p) = p^{a - 2a\beta} \int_{\mathbb{R}} \left(u^2 + 1 \right)^{-\beta} du,$$

which concludes the proof since $2a\beta - a = 2aH_1 + 1 = 2H_2 + 1$.

Following Definition 1 and combining Theorems 1 and 2 we obtain the following results as stated in Theorem 5.4 of [3].

Proposition 1 *For any direction $\theta = (\theta_1, \theta_2)$, the random field X admits H_1 for directional regularity in direction θ such that $\theta_1 \neq 0$. When $\theta_1 = 0$, the random field X admits H_2 for directional regularity in direction θ.*

The next section is devoted to the construction of estimators for H_1 and H_2.

2.3 Estimation

Generalized quadratic variations, studied in [14, 16], have been extensively used to estimate the Hurst parameter of a fractional Brownian motion. More generally they allow the estimation of critical Hölder exponents for Gaussian processes or fields. In [4] we give theoretical results of consitency and asymptotic normality for estimators based on generalized quadratic variations under asymptotic development of spectral densities assumptions. These results will be used in the context of this paper. Let us recall principles of these estimations. Let Y be a Gaussian process with stationary increments and a spectral density f. Let

$$\{Y(k/N); 0 \leq k \leq N\}$$

be an observed sequence. We consider the stationary sequence formed by second-order increments of Y with step $u \in \mathbb{N} \setminus \{0\}$

$$\forall\, p \in \mathbb{Z},\ Z_{N,u}(Y)(p) = Y((p+2u)/N) - 2Y((p+u)/N) + Y(p/N). \quad (11)$$

The generalized quadratic variations of Y of order 2 are then given by

$$V_{N,u}(Y) = \frac{1}{N-2u+1} \sum_{p=0}^{N-2u} \left(Z_{N,u}(Y)(p)\right)^2. \quad (12)$$

Let us quote that

$$\mathbb{E}(V_{N,u}(Y)) = \mathbb{E}((Z_{N,u}(Y)(0))^2) = \mathbb{E}\left(Y\left(\frac{2u}{N}\right) - 2Y\left(\frac{u}{N}\right) + Y(0)\right)^2,$$

According to Proposition 1.1 of [4], when $N \to +\infty$,

$$\mathbb{E}(V_{N,u}(Y)) \sim c_H N^{-2H} u^{2H},$$

for some $c_H > 0$, whenever the spectral density f satisfies $f(\xi) \sim c|\xi|^{-2H-1}$, when $|\xi| \to +\infty$, with $H \in \left(0, \frac{7}{4}\right)$ and $c > 0$. Intuitively, we can thus define an estimator of H as

$$\widehat{H}_{N,u,v} = \frac{1}{2\log(u/v)} \log\left(\frac{V_{N,u}(Y)}{V_{N,v}(Y)}\right). \quad (13)$$

In [14] the convergence of this estimator to H with asymptotic normality was shown under some appropriate assumptions on the variogram of Y. In Proposition 1.3 of [4], under assumptions on the spectral density, we prove that almost surely $\widehat{H}_{N,u,v} \longrightarrow H$, as $N \to +\infty$, with

$$\sqrt{N}\left(\widehat{H}_{N,u,v} - H\right) \xrightarrow{d} \mathcal{N}\left(0, \gamma_H^{u,v}\right), \text{ with } N\mathbb{E}\left(\left(\widehat{H}_{N,u,v} - H\right)^2\right) \to \gamma_H^{u,v}, \quad (14)$$

for some positive constant $\gamma_H^{u,v}$.

Now let us consider the 2-dimensional random field X and denote by $V_{N,u}(\theta)$ the variations of the line process $Y = X_{\theta,x_0}$ defined by Equations (5) and (12). Let

$$\hat{h}_{N,u,v}(\theta) = \frac{1}{2\log(u/v)} \log\left(\frac{V_{N,u}(\theta)}{V_{N,v}(\theta)}\right). \quad (15)$$

Theorem 3. *Let $\theta = (\theta_1, \theta_2)$ be a unit vector.*
(a) If $\theta_1 \neq 0$ and $\theta_2 \neq 0$, then $\hat{h}_{N,u,v}(\theta) \to H_1$, almost surely as $N \to +\infty$. Moreover, when $a > 2$, (14) holds for $H = H_1$.
When $a \leq 2$,

$$\mathbb{E}\left(\left(\hat{h}_{N,u,v}(\theta) - H_1\right)^2\right) = O_{N\to+\infty}\left(N^{-2(1-1/a)}\right).$$

(b) If $\theta_2 = 0$, then $\hat{h}_{N,u,v}(\theta) \to H_1$, almost surely as $N \to +\infty$. Moreover, (14) holds for $H = H_1$.
(c) If $\theta_1 = 0$, then $\hat{h}_{N,u,v}(\theta) \to H_2$, almost surely as $N \to +\infty$. Moreover, (14) holds for $H = H_2$.

Proof. Let $\theta = (\theta_1, \theta_2)$ be a unit vector. According to Proposition 1.3 of [4] results follow if $T_\theta f$, the spectral density of the process X_{θ,x_0} fulfills assumptions of Propositions 1.1 and 1.2 of [4]. We already know an asymptotic development for $T_\theta f$ from Theorem 2 such that Propositions 1.1 applies. The main additionnal assumption of Propositions 1.2 is concerned with (9) requiring an asymptotic development for the derivative of $T_\theta f$. However, it can be weakened by the following one: $T_\theta f$ is differentiable on $\mathbb{R} \setminus (-r, r)$, for r large enough and

$$(T_\theta f)'(p) = O_{|p|\to+\infty}\left(|p|^{-2H-2}\right), \quad (16)$$

with $H = H_1$ if $\theta_1 \neq 0$ and $H = H_2$ otherwise. It remains to check (16). Let us assume that $\theta_1 \neq 0$ and recall that from (10), for all $p \neq 0$,

$$T_\theta f(p) = \frac{1}{|\theta_1|}\int_{\mathbb{R}} \left(\left(p/\theta_1 + u\theta_2/\theta_1\right)^2 + u^{2a}\right)^{-\beta} du.$$

Therefore $T_\theta f(p)$ is differentiable on $\mathbb{R} \setminus \{0\}$ with

$$(T_\theta f)'(p) = -\frac{2\beta}{|\theta_1|\theta_1}\int_{\mathbb{R}} \left(p/\theta_1 + u\theta_2/\theta_1\right)\left(\left(p/\theta_1 + u\theta_2/\theta_1\right)^2 + u^{2a}\right)^{-\beta-1} du.$$

Let $p > 0$ and let the change of variables $u = p^{1/a}s$ such that

$$(T_\theta f)'(p) = -\frac{2\beta p^{1/a-2\beta-1}}{|\theta_1|\theta_1} \int_{\mathbb{R}} \left(\frac{1}{\theta_1} + \frac{s\theta_2}{\theta_1 p^{1-1/a}}\right) \left(\left(\frac{1}{\theta_1} + \frac{s\theta_2}{\theta_1 p^{1-1/a}}\right)^2 + s^{2a}\right)^{-\beta-1} ds.$$

Then, as in the proof of Theorem 2, one can show that

$$|(T_\theta f)'(p)| \leq \frac{2\beta p^{1/a-2\beta-1}}{\theta_1^2} \left(\int_{\mathbb{R}} \frac{3}{2|\theta_1|} \left(1/4\theta_1^2 + s^{2a}\right)^{-\beta-1} ds + \int_{|s|>1} s^{-a(2\beta+1)} ds\right).$$

This gives (16) with $H = H_1$, since $(T_\theta f)'$ is odd, $1/a - 2\beta - 1 = -2H_1 - 2$ and $a(2\beta+1) > 1$.
The remaining cases $\theta_1 = 0$ or $\theta_2 = 0$ are straightforward using (b) and (c) of Theorem 2.

3 Application to trabecular bone x-ray images

Results of [1] suggest that fractal analysis of trabecular bone radiographic images is a good indicator of the alteration of the bone microarchitecture. In association with bone mineral density, fractal analysis improves the fracture risk evaluation. However, since this analysis is based on an isotropic model, it does not reveal bone texture anisotropy which is of special interest for the diagnosis of osteoporosis [7, 9].

In this section, we apply our estimation methods to trabecular bone x-ray images. The database contains radiographs of 211 post menopausal women, 165 being control cases and 46 osteoporotic fracture cases. Radiographs were acquired at INSERM U658 (Orleans, France) using a standardized procedure [18]. They were obtained on calcaneus with a direct digital X-ray prototype (BMA$^{\text{TM}}$, D3A Medical Systems, Orleans, France) with focal distance 1.15 m and X-ray parameters 55 kV and 20 mAs. The high-resolution digital detector integrated into the device prototype had a 50 μm pixel size, providing a spatial resolution of 8 line pairs per millimeter at 10% modulation transfer function. For each subject, the software device selected a region of interest (ROI) of constant size $1.6 \times 1.6\text{cm}^2$ at a same position using three predefined anatomical landmarks localized by the operator ; see figure 1.

In each image of the ROI, we computed the quadratic variations on lines oriented in four different directions ((1) horizontal direction ($\theta = (1,0)$), (2) vertical direction ($\theta = (0,1)$), (3) first diagonal direction ($\theta = (1,1)/\sqrt{2}$), (4) second diagonal direction ($\theta = (-1,1)/\sqrt{2}$)) and at scales u ranging from 1 to 20 pixels (see Equations (5) and (12)). Log-log-plots of mean variations vs. scale are shown on Figure 2. Scale properties observed in direction 2 differ significantly from those in directions 1, 3 and 4, which are very close. The graph is almost a line in direction 2 (vertical) whereas it is curvilinear in the other directions.

In direction 2, images could be considered as self-similar from the smallest scale to the largest one. In other directions, the self-similarity property is not

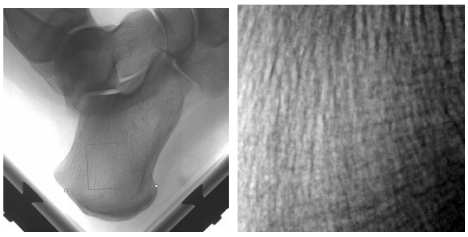

(a) (b)

Fig. 1. (a) ROI of the os calcis with anatomical landmarks and (b) a radiograph of the ROI.

valid considering all scales. This property is partially true on two consecutive scale ranges: a small scale range from 1 ($50\mu m$) to 5 pixels ($250\mu m$) and a large scale range above 5 pixels ($250\mu m$). The first range covers scales corresponding to the thickness of trabeculae in the calcaneus. The second range includes scales which are beyond the size of bone structures. In other words, in directions 1, 3, and 4, we can clearly distinguish the scaling properties inside structures from those between the structures. Besides, differences observed between scaling properties in direction 2 and in directions 1, 3 and 4 reflect the presence of longitudinal trabeculae, which are predominant structures in the calcaneum oriented in direction 2.

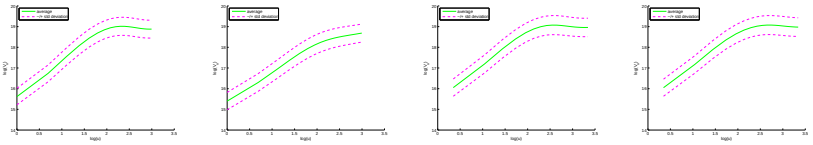

$\theta = (1, 0)$ $\theta = (0, 1)$ $\theta = (1, 1)/\sqrt{2}$ $\theta = (-1, 1)/\sqrt{2}$

Fig. 2. Plots of the logarithm of the quadratic variations V_u versus the logarithm of the scale u (in pixels) in different directions θ of the plane.

As described in Equation (15), we estimated the anisotropic index in the four directions on each image by comparing quadratic variations at scales $u = 6$ and $v = 5$ (pixels). On average, we obtained values 0.51 ± 0.08, 0.56 ± 0.06, 0.51 ± 0.08, and 0.51 ± 0.09 for directions 1, 2, 3, and 4, respectively. Comparisons of estimates in pairs of directions on each image are shown on Figure 3. They reveal that the anisotropic index is approximately the same in directions 1, 3, and 4 and higher in direction 2. This observation suggests that bone radiographs would have the same regularity in all directions except one (direction 2). From

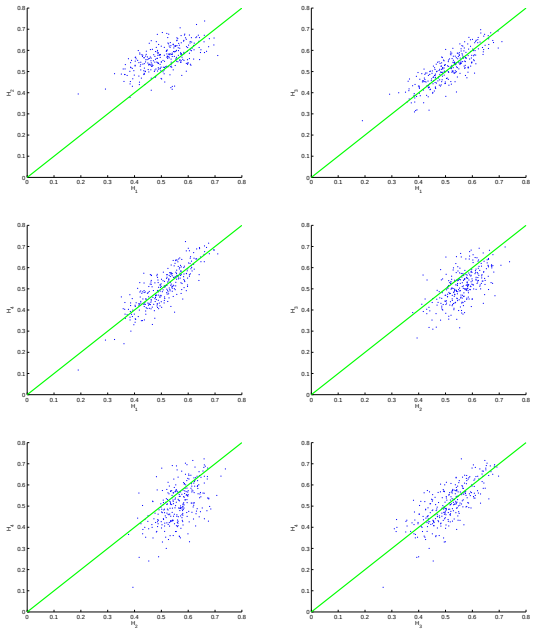

Fig. 3. Comparison of the anisotropic index estimation in pairs of directions. H_1, H_2, H_3 and H_4 are the estimation of the anisotropic index in directions $(1,0)$, $(0,1)$, $(1,1)$, and $(-1,1)$, respectively.

a theoretical point of view, such a property is consistent with the property of Gaussian operator scaling random fields proven in Theorem 2 of this paper.

4 Conclusion

In this paper, we studied some particular operator scaling fields which are anisotropic generalizations of the Fractional Brownian Field. We showed that they have a privileged direction where line restrictions are more regular than in other directions. We also constructed some techniques for the estimation of parameters of these fields, using line restrictions and following principles of generalized quadratic variations. We then proved the convergence of these estimators. We then modeled trabecular bone radiographs by operator scaling Gaussian random fields and showed experimentally that images had some properties of the model.

References

1. C.L. Benhamou, S. Poupon, E. Lespessailles, et al. Fractal analysis of radiographic trabecular bone texture and bone mineral density. *J. Bone Miner. Res.*, 16(4):697–

703, 2001.
2. D. Benson, M. M. Meerschaert, B. Bäumer, and H. P. Scheffler. Aquifer operator-scaling and the effect on solute mixing and dispersion. *Water Resour. Res.*, 42:1–18, 2006.
3. H. Biermé, M. M. Meerschaert, and H. P. Scheffler. Operator scaling stable random fields. *Stoch. Proc. Appl.*, 117(3):312–332, 2007.
4. H. Biermé and F. Richard. Estimation of anisotropic gaussian fields through radon transform. *ESAIM: Probab. Stat.*, 12(1): 30–50, 2008.
5. H. Biermé, F. Richard, M. Rachidi and C. L. Benhamou. Anisotropic texture modeling and applications to medical image analysis. *ESAIM: Proc.*, Mathematical methods for imaging and inverse problems, 2009.
6. A. Bonami and A. Estrade. Anisotropic analysis of some Gaussian models. *J. Fourier Anal. Appl.*, 9:215–236, 2003.
7. B. Brunet-Imbault, G. Lemineur, C. Chappard, et al. A new anisotropy index on trabecular bone radiographic images using the fast Fourier transform. *BMC Med. Imaging*, 5(4), 2005.
8. C. Caldwell, S. Stapleton, D. Holdsworth, et al. Characterisation of mammographic parenchymal patterns by fractal dimension. *Phys. Med. Biol.*, 35(2):235–247, 1990.
9. C. Chappard, B. Brunet-Imbault, G. Lemineur, et al. Anisotropy changes in post-menopausal osteoporosis: characterization by a new index applied to trabecular bone radiographic images. *Osteoporos Int*, 16: 1193–1202, 2005.
10. C.-C. Chen, J. Daponte, and M. Fox. Fractal feature analysis and classification in medical imaging. *IEEE Trans. Pattern. Anal. Mach. Intell.*, 8(2):133–142, 1989.
11. S. Davies and P. Hall. Fractal analysis of surface roughness by using spatial data. *J. R. Stat. Soc. Ser. B*, 61:3–37, 1999.
12. B. Grosjean and L. Moisan A-contrario detectability of spots in textured backgrounds *J. Math. Imaging Vis.*, 33(3):313–337, 2009.
13. J. Heine and P. Malhorta. Mammographic tissue, breast cancer risk, serial image analysis, and digital mammography: tissue and related risk factors. *Acad. Radiol*, 9:298–316, 2002.
14. J. Istas and G. Lang. Quadratic variations and estimation of the local Holder index of a Gaussian process. *Ann. Inst. Henri Poincaré, Probab. Statist.*, 33(4):407–436, 1997.
15. I. Karatzas and E. Shreve. Brownian Motion and Stochastic Calculus. Springer-Verlag, 1998.
16. J. T. Kent and A. T. A. Wood. Estimating the fractal dimension of a locally self-similar Gaussian process by using increments. *J. R. Stat. Soc. Ser. B*, 59(3):679–699, 1997.
17. A. N. Kolmogorov. Wienersche Spiralen und einige andere interessante Kurven in Hilbertsche Raum.. *C. R. (Dokl.) Acad. Sci. URSS*,26:115–118,1940.
18. E. Lespessailles, C. Gadois, G. Lemineur, J.P. Do-Huu, L. Benhamou. Bone texture analysis on direct digital radiographic images: precision study and relationship with bone mineral density at the os calcis. *Calcif. Tissue Int.*, 80:97–102, 2007.
19. B. B. Mandelbrot and J. Van Ness. Fractional Brownian motion, fractionnal noises and applications. *SIAM Rev.*, 10:422–437, 1968.
20. Y. Xiao. Sample path properties of anisotropic Gaussian random fields. In *A Minicourse on Stochastic Partial Differential Equations*, (D. Khoshnevisan and F. Rassoul-Agha, editors), Lecture Notes in Math. 1962, pp. 145–212, Springer, New York, 2009.